# Long wave antenna design for CALLISTO System

Supun Liyanaarachchi
*Astronomy and Space Science Division*
*Department of Physics, University of Colombo*
Colombo-03, Sri Lanka
supund2016@gmail.com

Janaka Adassuriya
*Astronomy Division*
*Arthur C Clarke Institute for Modern Technologies*
Katubedda, Moratuwa, Sri Lanka
adassuriya@gmail.com

K.P.S. Chandana Jayaratne
*Astronomy and Space Science Division*
*Department of Physics, University of Colombo*
Colombo-03, Sri Lanka
chandana@phys.cmb.ac.lk

2021 From Innovation To Impact (FITI) | 978-1-6654-8325-4/21/$31.00 ©2021 IEEE | DOI: 10.1109/FITI54902.2021.9833069

***Abstract*—Life on the surface of the earth is highly affected by solar activities. The real time observations of these solar activities are highly important to minimize the effect on the earth system. Solar radio observations are relevant to the study of such phenomena. The Compound Astronomical Low-frequency Low-cost Instrument for Spectroscopy and Transportable Observatory (CALLISTO) system is one method to study the solar radio bursts. This paper highlights a new study leading to the development of a long wave antenna (LWA) design, which is proposed for a new CALLISTO station. Generally, the solar radio bursts are circularly polarized and more often observed in low regions of the high frequency (HF) and very high frequency (VHF) bands. Therefore, the antenna is designed for the frequency range of 20 MHz to 100 MHz. The designing of the antenna was done using 4nec2 software, a Numerical Electromagnetics Code (NEC) based antenna modeller and an optimizer. The main structure of the design contains two identical antennas in both north-south and east-west directions. The performance of the design was tested by changing the dimensions and simulating the model to optimize the parameters. Considerable performance increases could be observed by applying the ground plane to the antenna model. The resulting performance by simulation shows average gain test (AGT) values of 1.923 at 15 MHz, 2.001 at 30 MHz, 2.021 at 50 MHz, 2.056 at 70 MHz and 2.096 at 100 MHz. The 1.90 - 2.10 AGT range ensures the model is perfect with the input parameters for the physical production. The maximum gain was obtained as 9.12 dB at 50 MHz and in the frequency range considered, this design could maintain a gain higher than 7 dB. The other important performance factors, voltage standing wave ratio (VSWR), structure loss, efficiency, left-hand circular polarization (LHCP) and right-hand circular polarization (RHCP) gain, etc. are also observed. From the simulations, it was observed that LHCP gain is always dominating total gain.**

***Keywords—Solar Radio Burst, Circular Polarization, CALLISTO, Long Wave Antenna***

## I. INTRODUCTION

As the single and ultimate energy source of our solar system, the Sun causes many events affecting the whole solar system. These energetic events are yet unknown physical processes that are being studied under Solar Astronomy. Solar flares are one of these solar activities, and these affect the earth via the eruption of electromagnetic radiation. Multi-wavelength electromagnetic radiation emission processes of solar fares are observed and analyzed to model the emission processes. Solar radio bursts are radio emissions of solar flares observed in the radio window.

Analyzing the solar radio flux through the detection of solar radio bursts is the latest way of monitoring the sunspots, coronal mass ejection (CME), and solar activities. Grote Reber was the first to discover solar radio emissions in 1944 [1]. However, in 1942 during World War II the earliest solar radio phenomenon was detected, and it was a low-frequency radio wave. However, this observation was not reported until the end of the war as this was useful for dodging enemy radar signals [2]. Observations of solar radio bursts are made using antennas and the radio frequencies are recorded with the intensity. The radio spectrographs consist of a dynamic spectrum which is contiguously recording intensities of radio flux over a range of frequencies. Observations and data collections are carried out by using spectrometers in the Radio Solar Network, WAVE instrument on the Wind spacecraft and the e-CALLISTO network.

The CALLISTO spectrometer is a receiver instrument, which was designed by the Radio Plasma Physics Group from ETH Zurich, Switzerland [3]. CALLISTO observes the solar radio frequencies with its integrated antenna system and uploads the spectra to the main server in Switzerland. The CALLISTO is a system consisting of a programmable heterodyne receiver which needs an antenna system to grab the radio frequencies emitted by the sun. The solar radio bursts have the most probable frequency range of 10 MHz to 1000 MHz; the CALLISTO is designed to receive the frequency range between 45 MHz to 870 MHz.

## II. THE NEW CALLISTO STATION

The existing CALLISTO station at the Arthur C Clarke Institute (ACCIMT) is designed to receive plane-polarized signals of solar radio bursts [4]. The north-south direction log-periodic antenna only receives plane-polarized radio signals. Usually, the solar radio bursts are circular polarized and therefore the existing system cannot detect the entire radio burst. The proposed system has a Long Wave Antenna (LWA) system which has two identical antennas in both north-south and east-west directions and is connected to two CALLISTO receivers. The new system is designed for the range 20 MHz to 100 MHz. This range is decided with reference to Table I [5]. The most common types of solar radio burst types are Type II and Type III. The typical frequency distribution of Type II and Type III is 10 MHz to 200 MHz. Therefore, the new system is designed for the optimum range of 20 MHz to 100 MHz.

The entire system consists of developing an antenna and producing necessary radio frequency (RF) circuit components. Fig. 1 shows the schematic of the entire system.

Here we report only the design and performance of the LWA antenna design for the CALLISTO spectrometer. The report includes the antenna design, optimization, simulated results, and a suggestion to increase the gain of the system.

## III. ANTENNA DESIGN

The long wave crossed dipole array antenna is an inverted-V, tied fork design receiver with 4 triangular slop wings.

978-1-6654-8325-4/21/$31.00 ©2021 IEEE

TABLE I. SUMMARIZED DETAILS OF SOLAR RADIO BURSTS CLASSIFICATION

| Type | Duration | Frequency Bandwidth |
|---|---|---|
| **I** | Single burst ≈ 1 second, Noise storm for hours or days | 50-500 MHz |
| **II** | 3-30 minutes | 20-150 MHz |
| **III** | Single burst 1-3 seconds, Group 1-5 minutes, Storm minutes-hours | 10 kHz – 1 GHz |
| **$IV_s$** | Hours - days | 20 MHz – 2 GHz |
| **$IV_m$** | 30 – 120 minutes | 20 – 400 MHz |
| **V** | 1 – 3 minutes | 10 – 200 MHz |

The design was created according to the frequency range and the polarization (dipole). The software 4nec2 was used to model and simulate the design. This allowed us to model antenna based on Numerical Electromagnetics Code public domain version 2 (NEC-2) which was originally written in FORTRAN. Here, NEC-2 was used instead of using the latest versions, NEC-3 or NEC-4, as those require a license agreement with Lawrence Livermore National Laboratory.

We focused on developing a lower cost and higher-performance antenna than the model available for purchase. Using numerical simulations of the antenna design and considering its parameters, it was possible to recognize that an active dipole antenna is suitable for this purpose. Then by adding a conductive ground plane under the designed antenna, good performance by simulations was obtained. A simple sketch of the antenna is shown in Fig. 2.

The frequency range, 20 -100 MHz, the dimensions of the dipoles and triangular-shaped wings were obtained using antenna theory. By taking the average frequency as 50 MHz, the wavelength was determined as 5.995 m. Antenna lengths were calculated as nearly 2.58 m. All the dimensions of the antenna design are shown in Fig. 3. For the simulations, real ground parameters of 4nec2 software were used. In the design, the wings of the antenna had to slope downward at 50° as it improves the sky coverage. The antenna structure was planned to be developed using 30 mm square aluminum tubes which can be found easily. But the model was designed using 30 mm (diameter) round aluminum wire elements, as the 4nec2 accepts only round wires. The conductivity of 6061-T6 aluminum was set as the conductivity of the model in the simulation process.

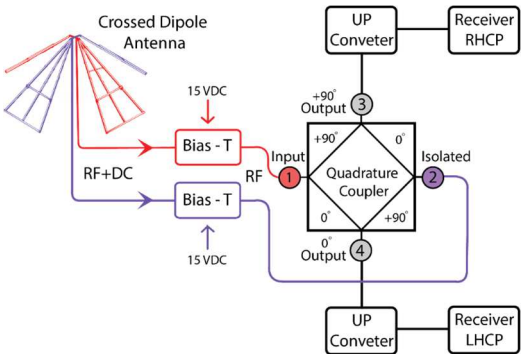


Fig. 1. The schematic design of the proposed antenna system is shown here. The antenna is phase 1 and the front end electronic (FEE) circuit is phase 2. Bias-T is used to inject DC currents or voltages into RF circuits without affecting the RF signal through the main transmission path. This can operate over a range of signal frequencies. Here DQK-10-100S hybrid coupler is used as the quadrature coupler.

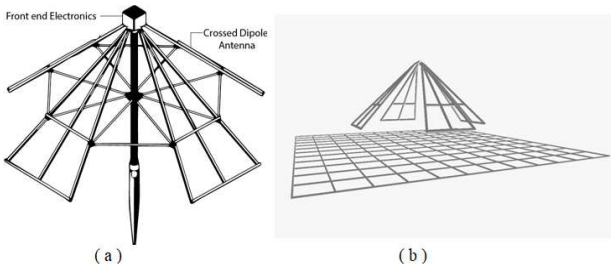


Fig. 2. (a) proposed antenna is shown and here the FEE circuit is placed in a box which is situated at the top of the antenna. Only wings and ground planes are made of metal and other elements are made of non-conducting material which is resistive to water and wind. The enclosure of FEE is also proposed to be produced using aluminum to avoid the effect of external RF signals. (b) Antenna model designed using 4nec2. The ground plane is also shown here.

### *A. The framework of the proposed Antenna*

For the designing process of the proposed antenna for the CALLISTO, all the steps were taken related to the features of the 4nec2 software and NEC file format. First, the dimensions of the reference antenna were obtained and modelled [6]. When modelling, all the main length values were assigned for variables and then the design was created using those variables. By changing the variables, frequency sweep and far-field pattern were generated. Using generated plots, gain vs frequency, SWR vs frequency, reflection coefficient vs frequency and the value of the average gain test, we checked whether the model is acceptable. After doing many tests, a good model was generated. TABLE II shows the variables, used for the model.

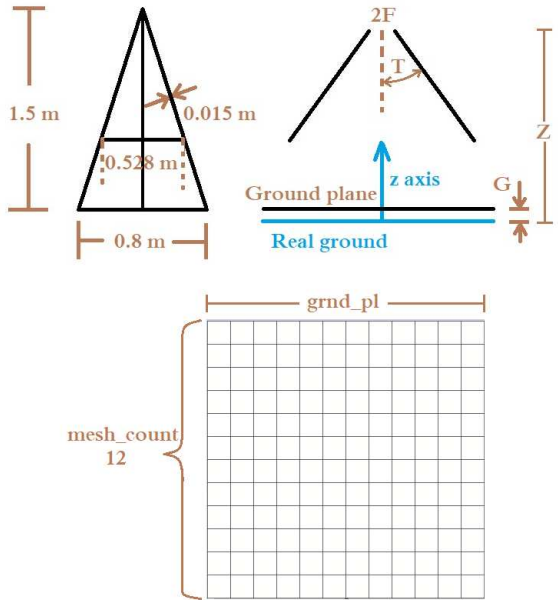


Fig. 3. Dimensions of a wing of the antenna (top left) and the front projection of the antenna (top right). Structure of the ground plane (bottom). [Parameters are mentioned in Table II. Dimensions are not to scale.] Here it is proposed to place the FEE between the wings and the best performance was obtained for a distance of nearly 20 cm. The PCB design was created according to this distance. We observed that this distance greatly affected the performance.

TABLE II. VARIABLES USED IN THE DESIGN

| Used symbol | Value[a] | Comment |
|---|---|---|
| Z | 1.44 | Height of the top of the antenna from the ground. |
| L | 1.00 | This variable is set as the common variable for lengths. All lengths are set according to this variable. |
| A | 0.015 | The radius of the wires segments which was used for the antenna structure (not for the ground plane) |
| r | 0.002 | The radius of the wire segments of the ground plane. |
| T | 50 | The angle between wings and the z-axis. |
| F | 0.099 | The minimum distance between the top edge of a wing to the z-axis. |
| grnd_pl | 3.6 | Length of one side of the ground plane |
| mesh_count | 12 | Number of mesh on one side of the plane |
| G | 0.01 | Height of the ground plane from the ground. |

[a.] All the measurements are in meters. (m)

The ground screen was used for stabilizing the environment and simulated for both large and small grounds and the final design was created using a 3.6 m × 3.6 m ground plane. The mesh density is not important if the lattice spacing is less than 12 inches (nearly 30 cm) [7]. With reference to this, 12 lattice spacings were used and one side length of a lattice is 30 cm. It needs to be noted that all simulated results are based on the "average" earth ground derived from Sommerfeld-Norton which is mentioned as the "real" earth ground model. For the ground plane, 4 mm (diameter) rounded wire segments were used. The plane is modelled 1 cm above the ground surface as NEC-2 does not allow wires to be embedded in the earth surface.

## IV. PERFORMANCE OF THE DESIGN

All the plots under this section are the results given by the 4nec2 software. Results of circular polarization are given with left-hand polarization, right-hand polarization, and the total of both polarizations. When checking the performance of NEC models, the average gain test plays a major role. The average gain test is the ratio of the power in the far-field to the power delivered to the antenna by the sources [7]. For a perfect antenna, the model must be 2.0 for the average gain test and, for a very good antenna model it must be 2.00 ± 0.10. Here in this model, we obtain average gain test value 1.923 at 15 MHz, 2.001 at 30 MHz, 2.021 at 50 MHz, 2.056 at 70 MHz and 2.096 for 100 MHz. These are the results that were obtained by the simulations, and it should be noted that the average gain test is not enough to conclude that the actual antenna is very good in performance.

The performance of the design also depends on the dimensions of the antenna elements. Fig. 3 shows the dimensions which gave a good performance for the design.

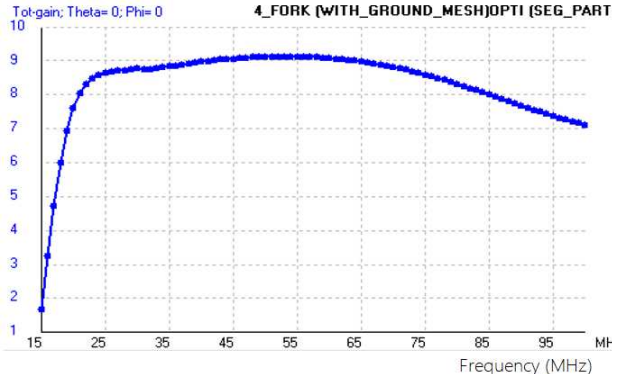


Fig. 4. Total gain for each frequency in the considered frequency range (with 1 MHz resolution). Maximum gain 9.12 can be seen at 54 MHz. At 100 MHz, the gain is 7.11 and near 20 MHz it is 7.61.

Under these dimensions, the gain was observed and at 15 MHz the gain is very low value, but at 20 MHz it shows more than 7 dB and for 50 MHz it reaches the maximum of 9.12 dB. Therefore, the gain is not less than 7 in the considered frequency range of 20 MHz-100 MHz (Fig. 4). Two-dimensional elevation plots, azimuth plots and 3-dimensional radiation patterns, near field plots, are also can be generated using 4nec2. According to the elevation pattern plots, a maximum of nearly 29 dB of difference between right-hand and left-hand polarization can be observed. Fig.5 shows elevation plots for 15 Mhz, 50 MHz and 100 MHz. We can observe that LHCP is the main polarization factor that affects the total polarization as the maximum difference between LHCP and RHCP is near, 25 dB at 15 MHz, 29 dB at 50 MHz, and 24 dB at 100 MHz. Fig. 6 shows the azimuth pattern or the omnidirectional characteristics. Here it shows that half-power beamwidths in elevation for the plotted frequencies are nearly 60°- 100°.

It is very important to match the antenna to the characteristic impedance of the feed line, for a maximum power transfer from the antenna. Due to the difficulties of achieving overall matching conditions for the impedance, matching networks should be used. Table III shows the simulation results for the required components for low pass and high pass networks, L, Pi and T.

TABLE III. RLC MATCHING VALUES FOR THE RF MATCHING METWORK

| **Characteristic Impedance** | **50 Ω** | **Frequency** | **50 MHz** |
|---|---|---|---|
| 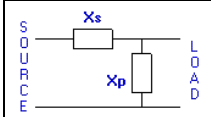 | **L-network** | | |
| | | Low-pass | High-pass |
| | Xs | 380 $nH$ | 26.7 $pF$ |
| | Xp | 35.9 $pF$ | 1.07 $\mu H$ |
| 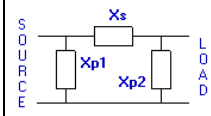 | **Pi-network** | | |
| | | Low-pass | High-pass |
| | Xp1 | 8.32 $pF$ | 1.22 $\mu H$ |
| | Xs | 398 $nH$ | 25.5 $pF$ |
| | Xp2 | 36.1 $pF$ | 1.05 $\mu H$ |
| 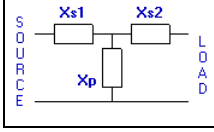 | **T-network** | | |
| | | Low-pass | High-pass |
| | Xs1 | 384 $nH$ | 26.4 $pF$ |
| | Xp | 35.7 $pF$ | 284 $nH$ |
| | Xs2 | 6.51 $nH$ | 9.96 $pF$ |

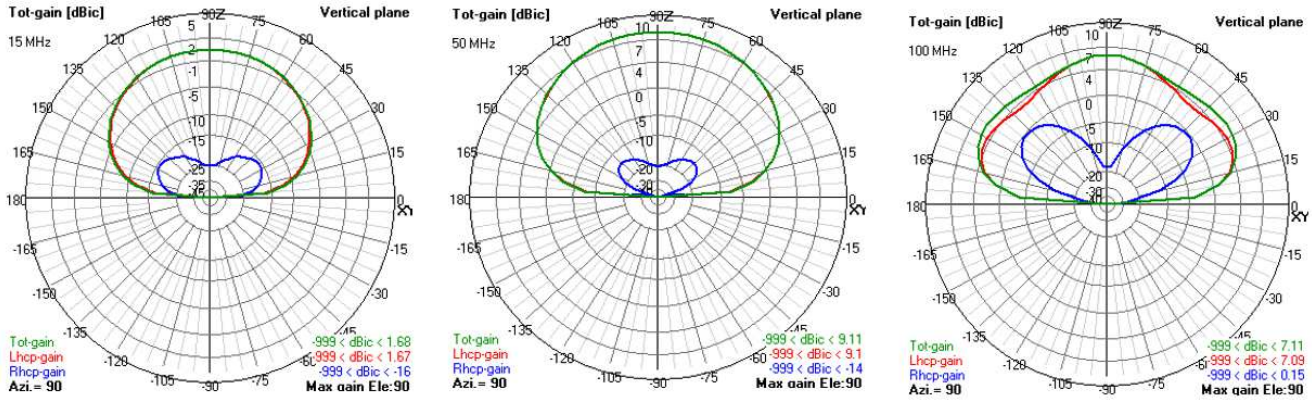


Fig. 5. Elevation plots for 15 MHz, 50 MHz and 100 MHz. Red color plot shows the gain of LHCP, blue is RHCP, and the total is shown by green color plot. The difference between the RHCP and LHCP is shown, and LHCP is dominating here.

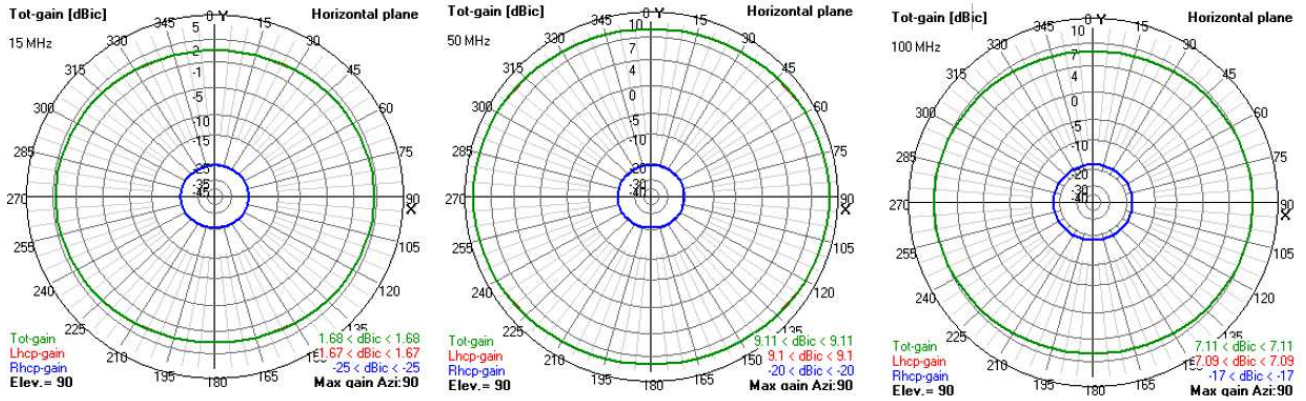


Fig. 6. Horizontal plane antenna pattern or the azimuth plot for 14 MHz, 50 MHz and 100 MHz. This shows the omnidirectional response of the antenna in azimuth. For all the frequencies the shape is common. Here also the red line which is overlapped by the green line shows the LHCP and the blue line shows RHCP, while the total gain is shown by the green line.

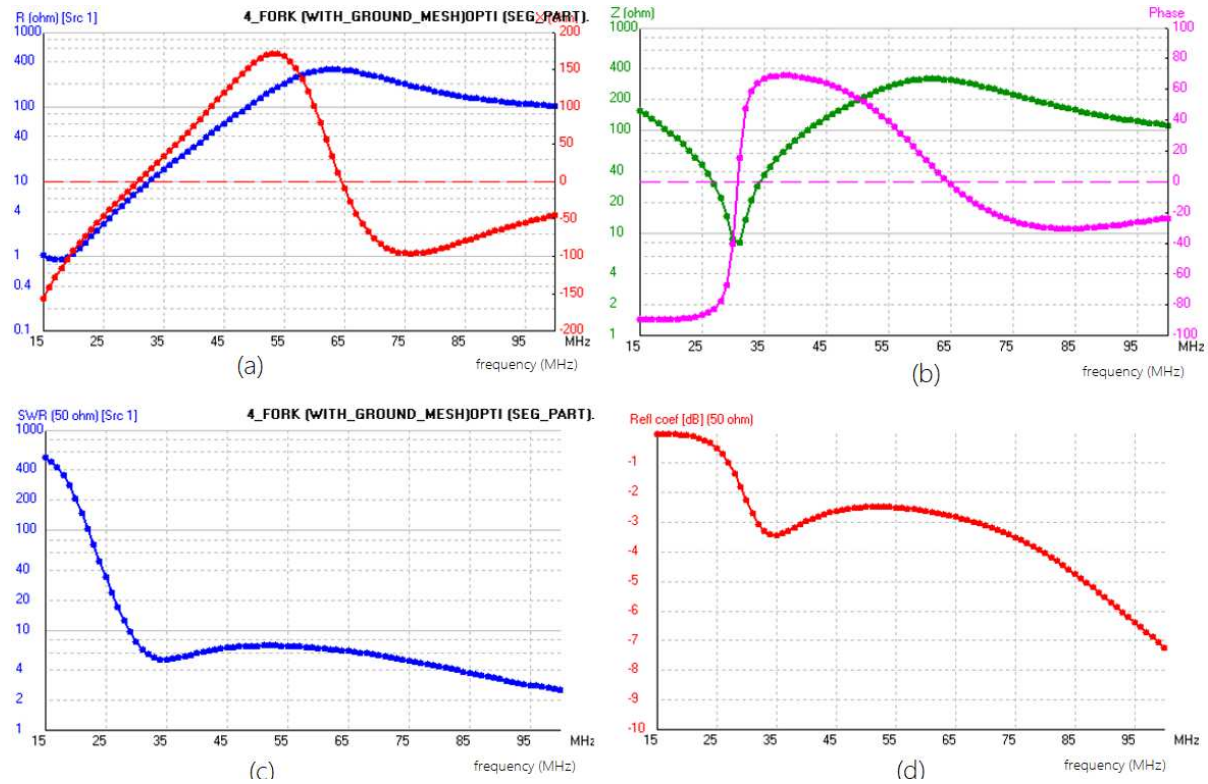


Fig. 7. (a) and (b) Resulting impedance of the crossed-dipole antenna model in the frequency range 15 MHz to 100 MHz. (c) SWR value for each frequency in the range. (d) The reflection coefficient of the antenna model is varying in the acceptable range.

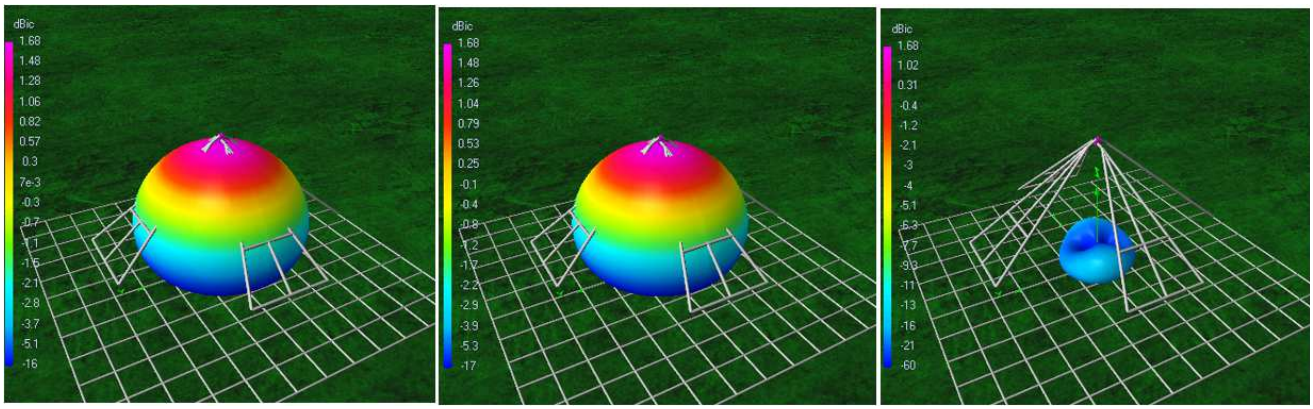


Fig. 8. 3-dimensional response pattern at 15 MHz. Left to right: Total gain, LHCP, and RHCP

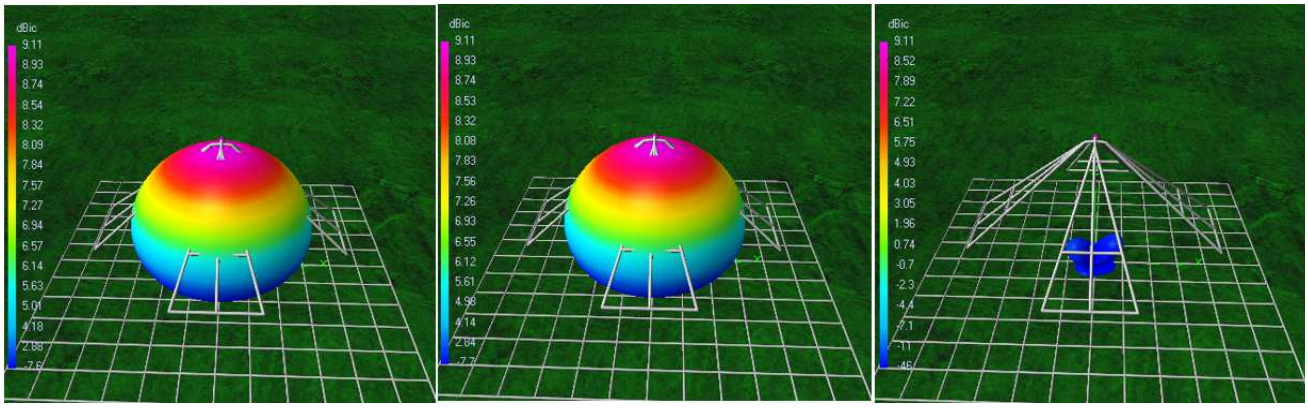


Fig. 9. 3-dimensional response pattern at 50MHz. Left to right: Total gain, LHCP, and RHCP

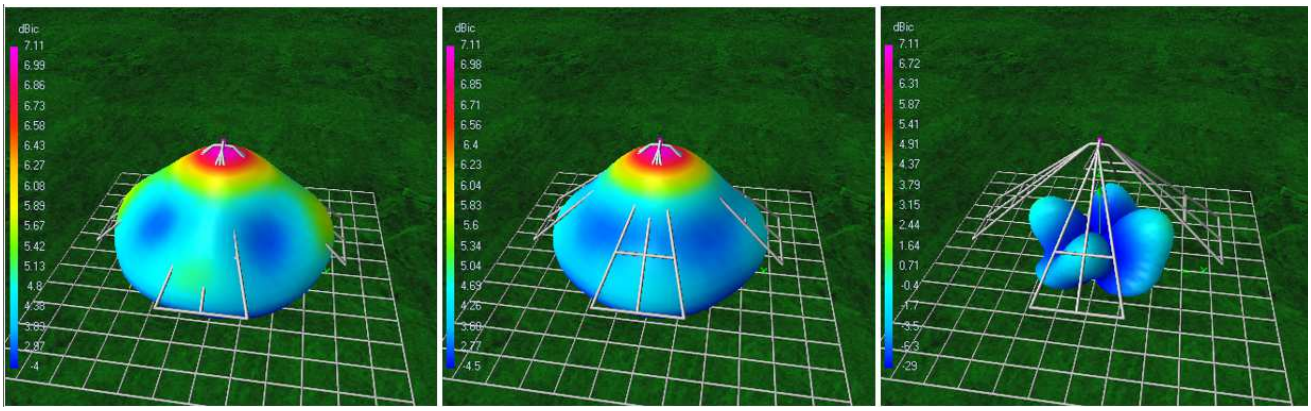


Fig. 10. 3-dimensional response pattern at 100 MHz. Left to right: Total gain, LHCP, and RHCP

## REFERENCES


[1] G. Reber, 1940. Cosmic Static. Proceedings of the IRE, 28(2), pp.68-70.

[2] J.S. Hey, 1946. “Solar radiations in the 4–6 metre radio wave-length band,” Nature, 157, pp.47-48.

[3] A. Benz, C. Monstein, and H. Meyer, H., 2005, “A new concept for solar radio spectrometers,” in Solar Physics, 226(1), pp.143-151.

[4] J. Adassuriya, S. Gunasekera, K.P.S. Jayaratne, and C. Monstein, 2014. “Observation of solar radio bursts using e-callisto system”.

[5] R.K. Sasikumar, P. Subramanian, S. Ananthakrishnan, and C. Monstein, 2018. “Callisto spectrometer at IISER-pune," arXiv:1801.03547

[6] W.J. Robbins, H.R. Schmitt, P.S. Ray, and N. Paravastu, 2009. “Simulations and Final Choice of Ground Screen Material,” LWA Engineering Memo GND0005 (http://www.ece.vt.edu/swe/lwa/)

[7] Reeve.com. 2021. [online] Available at: <https://reeve.com/Documents/Long%20Wavelength%20Array/Reeve_LWA-Model.pdf>